



Mechanical and optical characteristics of multilayer inorganic films on polyimide for anti-atomic-oxygen erosion

Yongxian Huang^{a,*}, Xiubo Tian^a, Shixiong Lv^a, Ricky K.Y. Fu^b, Paul K. Chu^b

^a State Key Laboratory of Advanced Welding and Joining, Harbin Institute of Technology, Harbin 150001, People's Republic of China

^b Department of Physics and Materials Science, City University of Hong Kong, Tat Chee Avenue, Kowloon, Hong Kong

ARTICLE INFO

Article history:

Received 2 February 2012

Received in revised form 20 February 2012

Accepted 21 February 2012

Available online 3 March 2012

Keywords:

Polyimide

Multilayer

Inorganic films

Erosion

Optical properties

ABSTRACT

Multilayer inorganic silica/alumina films with excellent mechanical, optical and anti-atomic-oxygen erosion characteristics were fabricated by the hybrid implanting and depositing processes of Al/Si plasmas on polyimide. The multilayer films exhibited an excellent mechanical stability, demonstrating that balanced internal stresses and alternating bonding structures were crucial for enhancing mechanical stability. The multilayer inorganic films exhibited higher optical transmittance. The slight change surface morphology and high mechanical stability of polyimide covered with multilayer silica/alumina films suggest that the technique used is an effective method to protect polymer materials which are applied to thermal control system of spacecrafts in low Earth orbit.

© 2012 Elsevier B.V. All rights reserved.

1. Introduction

Numerous satellites are being launched into low Earth orbit (LEO) altitudes, ranging from 200 to 700 km. A large portion of the structure of such satellites comprises high-performance polymeric materials, thanks to their lightweight and unique properties. For example, polyimides (PIs) are widely used as matrix resin of composite materials, friction material, optical materials, thermal controlling materials and power system materials in aerospace industries because of their outstanding tensile strength and modulus, excellent thermal stability and dielectric properties [1]. However, polymer materials exposed directly to a LEO environment can collide with atomic oxygen (AO) at spacecraft velocities of about 8 km/s. The translational energy of the AO collisions is approximately 5 eV, which is sufficient to break the polymer bond and induce oxidative decomposition [2]. The interaction of AO with PIs located at the outer surfaces of a spacecraft may result in their degradation and mass loss, thereby affecting their chemical, electrical, thermal, optical and mechanical properties [3,4]. Owing to some unique properties such as optical transparency, high thermal/mechanical resistivity and high electrical properties, inorganic

oxides have been used in a variety of electronic, biological, structural devices and anti-AO erosion [5–7].

Recently, to protect against AO erosion of polymer, the need for functional inorganic oxide films is rapidly increasing, and the mechanical stability of inorganic thin films is inevitably becoming important for applications, particularly in long duration LEO missions such as the International Space Station (ISS). In general, inorganic oxide thin films can be fabricated on a substrate by sputtering, chemical vapor deposition (CVD), atomic layer deposition (ALD), laser ablation and sol-gel coating [8–10]. Moreover, depending on the fabrication process, the extrinsic properties of inorganic oxide thin films are significantly changed by defects such as pinholes or cracks introduced during manufacture [5]. Organic–inorganic hybrid nanocomposites have received extensive interests from both the academic and the industrial societies. Organic–inorganic hybrid polyimide films such as PI/SiO₂ [11], PI/Al₂O₃ [12–14] and PI/V₂O₅ [15] have been widely reported. Moreover, some of them have been evaluated as AO resistant films. Especially, alumina and silica films are attracting considerable scientific attention. Due to the fact that such coatings offer excellent AO erosion resistance, properties which are particularly important for long term space applications. Silica/alumina films have high transparency, tunable refractive indexes by adjusting composition, low loss in transporting process, and high chemical durability [16,17]. The combination of silica and alumina also gives the ability to improve mechanical properties and to extend the wear life [18]. It is possible to fabricate multilayer inorganic silica/alumina films with high mechanical stability on PIs for anti-AO erosion.

* Corresponding author at: State Key Laboratory of Advanced Welding and Joining, Harbin Institute of Technology, No. 92, West Da-Zhi Street, Harbin 150001, Heilongjiang, People's Republic of China. Tel.: +86 451 86413951; fax: +86 451 86416186.

E-mail address: yxhuang@hit.edu.cn (Y. Huang).

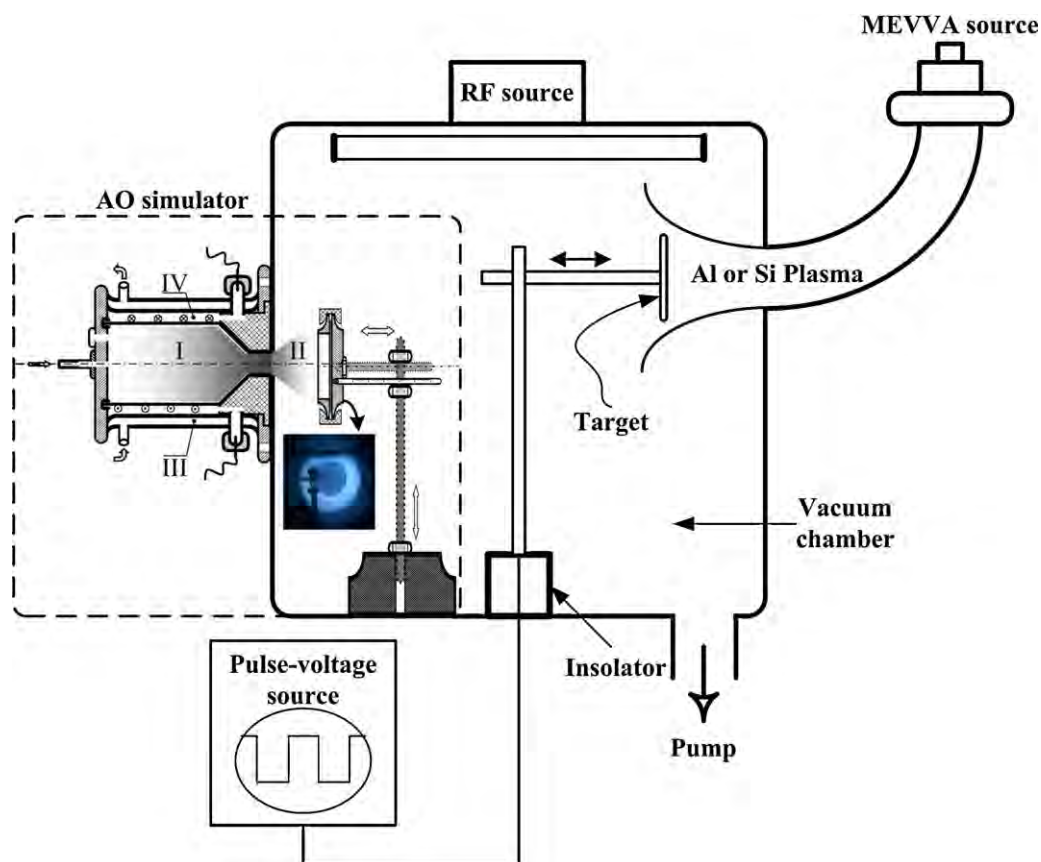


Fig. 1. Schematic diagram of the experimental apparatus for the fabrication of multilayer inorganic silica/alumina films on polyimide with the dashed lines denoting the AO simulator.

The aim of this study is to obtain multilayer inorganic silica/alumina films on polyimide, with attention to their outstanding mechanical, optical and anti-AO erosion performances. This work exploits a hybrid approach in a deposition and implantation way, to create high-quality multilayer inorganic films at low temperature. This approach offers a great flexibility for inorganic films design, with the capability to provide mechanical, optical and anti-AO erosion properties.

2. Experimental

2.1. Materials and preparation of silica/alumina films

Experiments were performed with 100 μm thick polyimide film (DuPont™). The starting materials were a solid aluminum target (99.99 at.%) and a silicon target (99.99 at.%). High purity oxygen was used as reactive gas. Multilayer inorganic silica/alumina films were fabricated on the surface of polyimide using filtered vacuum arc plasma ion implantation and deposition (FVAPIID), as shown in Fig. 1. Spring steel clips covered with aluminum foil were utilized to provide a tight contact of the polyimide sample with the aluminum stage to prevent arcing or sparking during FVAPIID. The polyimide samples with the size of 100 mm \times 100 mm were positioned 15 cm away from the exit of the curved filtered duct. Before plasma ion deposition and implantation, the polyimide sample was immersed in hydrogen plasma sustained by radio frequency (RF, 13.56 MHz) source with power of 500 W and gas pressure of 1.4×10^{-4} Torr for 30 min. After then, the sample was biased to a negative pulse bias of 10 kV with pulse width of 150 μs and repetition rate of 60 Hz. The

aluminum and silicon plasmas were generated from the vacuum arc using a high voltage to trigger the metal arc and a low sustaining arc voltage between the cathode and anode. The chamber was evacuated to a base pressure of 2.4×10^{-4} Torr. The polyimide samples were treated in the Al plasma for 60 min and then in Si plasma for 60 min. The pulse duration of bias was 150 μs while the arc plasma was maintained with the duration of 300 μs . This approach could achieve hybrid processes with implantation and deposition, and the processes could enhance the adhesion strength due to the ion bombardment effect. The highest temperature of sample stage is about 80 $^{\circ}\text{C}$ measured by thermocouple during the processes.

2.2. AO exposure tests

Polyimide covered with multilayer inorganic silica/alumina films were exposed to an oxygen RF inductively coupled plasma environment, simulating the effect of AO in the LEO. A conventional RF plasma reactor (1000 W, 13.56 MHz), operating at 1.5 Pa of oxygen and 400 W of RF power, was used to simulate the exposure of AO in the same vacuum chamber, as shown in Fig. 1. The sample was located 45 mm downstream from the reactor, in the afterglow region, where it was exposed to a mixture of atomic and molecular oxygen, excited species and vacuum UV (VUV) radiation. Nevertheless, the contribution of ions, VUV and excited species is reduced compared to the RF plasma reactor environment [19,20]. And the exposing temperature is about 50 $^{\circ}\text{C}$ which is much lower than the softening and glass-transition temperatures of the polyimide. Detailed introductions to the system configuration and operating characteristics of the ground-based AO effects experimental system

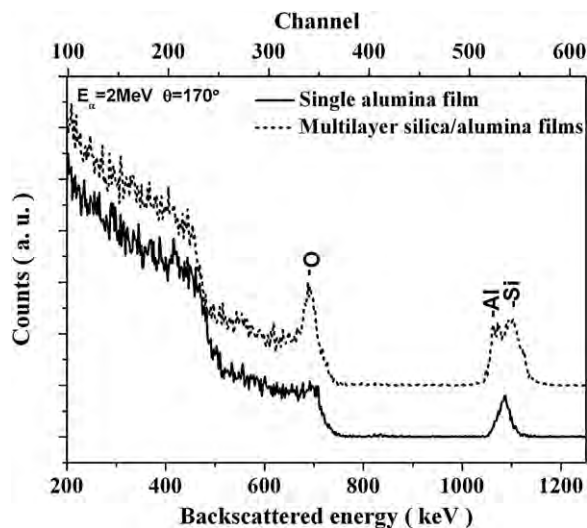


Fig. 2. RBS spectra of the single alumina film and multilayer silica/alumina films on the polyimide substrate.

are available in our previous work [21]. According to the following equation to calculate the effective AO flux, f_k [22]:

$$f_k = \frac{\Delta M_k}{A_k \rho_k E_k t}, \quad (1)$$

where ΔM_k is the mass change (g), A_k is the exposed area of (cm^2), ρ_k is the density (g/cm^3), E_k is the erosion yield of the Kapton in space ($3 \times 10^{-24} \text{ cm}^3/\text{atom}$), and t is the exposure time (s).

2.3. Characterization techniques

Rutherford backscattering spectrometry (RBS) was performed using 2 MeV $^4\text{He}^+$ and a backscattered angle of 170° to provide the composition for the nanometer-thick foils. X-ray photoelectron spectroscopy (XPS) was performed on the Physical Electronics PHI-5600 using the monochromatic Al K α radiation operated at 14 kV and 350 W. The photoelectron takeoff angle was 45° . The morphologies were examined by scanning electron microscopy (SEM, Hitach S-4700), operated at 15 kV. The samples were deposited with Pt in preparation for SEM observation. Mechanical folding tests were undertaken to determine the cohesion and adhesive properties of the thin films on the polymer substrate. The evolution of crack behaviors of the inorganic film is monitored.

3. Results

3.1. Chemical composition of multilayer structures

The RBS spectra of the alumina film and multilayer silica/alumina films on polyimide are depicted in Fig. 2. The aluminum and silicon signals are detected at a backscattered energy of around 1100 keV. This indicates the formation of multilayer silica/alumina films on polyimide substrate. The result means that the implanted Si ions may change the alumina to a new material $\text{Al}_2\text{O}_3 \cdot \text{SiO}_2$ [23]. It is also reported that Al atom tends to react with SiO_2 when a silicon oxide layer is present on their surface [24].

The element concentrations of C, O, N, Al and Si calculated from Fig. 3 are shown in the inset table. Clearly, the alumina film has been produced on the surface of polyimide, where, the relative concentration of C decreases from 78.9% to 40.7% and N from 7.6% to 2.9%, while the relative concentration of O increases from 13.6% to 41.2%, and the concentration of Al is up to 15.3%. It implies that the implanted/deposited aluminum plasma has been oxidized to form

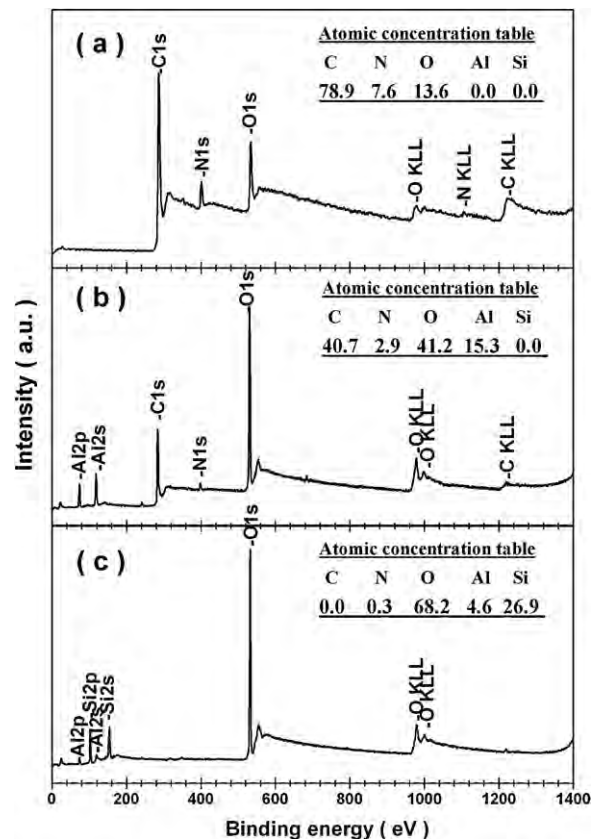


Fig. 3. XPS spectra showing the elemental concentration: (a) control polyimide surface, (b) single alumina film surface, and (c) multilayer silica/alumina films surface.

alumina. When the multilayer silica/alumina films are formed, the carbon and nitrogen contents are nearly zero, while the silicon content increases to 26.9% and the aluminum content decreases to 4.6% as shown in Fig. 3(c). On the multilayer silica/alumina films surface, the concentrations of Si, Al, O accord with stoichiometric of SiO_2 and Al_2O_3 , indicating that multilayer silica/alumina films are formed on the polyimide substrate.

3.2. Adhesive properties analysis

The crack resistance is very important for protective films since AO erosion can easily proliferate when the film is damaged [25]. A mechanical folding test is performed to assess the crack behavior of the multilayer silica/alumina films on polyimide. The typical fracture surface after five cycles folding test with open angle of 180° is shown in Fig. 4. The inset of Fig. 4 illustrates schematically the folding test with a bidirectional folding angle of 180° . The cracks may initiate due to the folding-induced stress and the cracks spread perpendicularly to the folding direction. After five cycles folding test, flaking morphology is invisible with the exception of micro-cracks only at the high distortion zone with the width less than $400 \mu\text{m}$. This means better adhesion between the inorganic films and polymer substrate between different layers. Therefore, the FVAPIID method can be used to produce high adherent and crack-free multilayer inorganic silica/alumina films on polyimide.

3.3. Optical properties analysis

The optical properties were measured using a Perkin-Elmer Lambda 2s UV/VIS spectrophotometer with wavelength ranging from the near-infrared to ultraviolet, and in more detail in the red (700 nm wavelength). All measurements were made in the

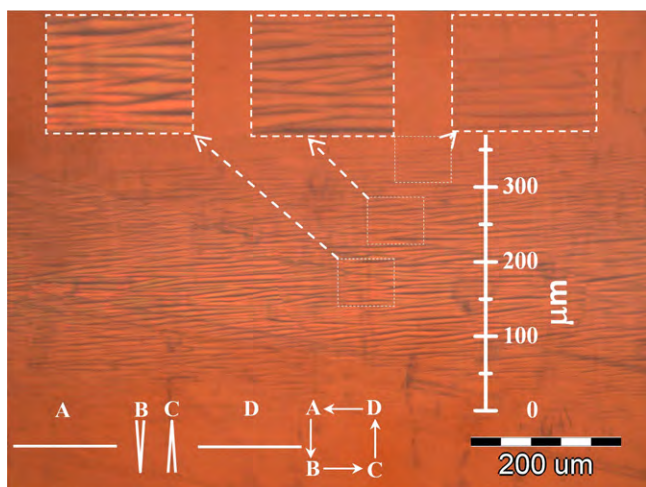


Fig. 4. Optical micrograph showing cracks on the multilayer silica/alumina films after folding test with the inset presenting a schematic diagram of the mechanical folding test.

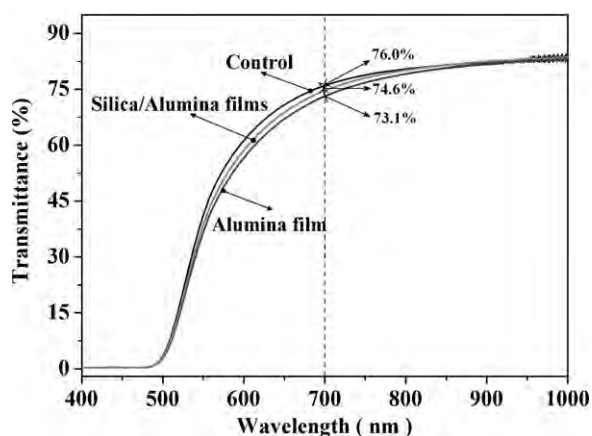


Fig. 5. Optical transmittance of polyimide samples covered with inorganic films with gas background measurement.

laboratory in air and at room temperature. The optical transmittance of differing films on polyimide film is shown in Figs. 5 and 6 with different background measurements. The untreated polyimide foil shows high transmittance in the near-infrared and visible region as well as total absorption in the UV region. At a

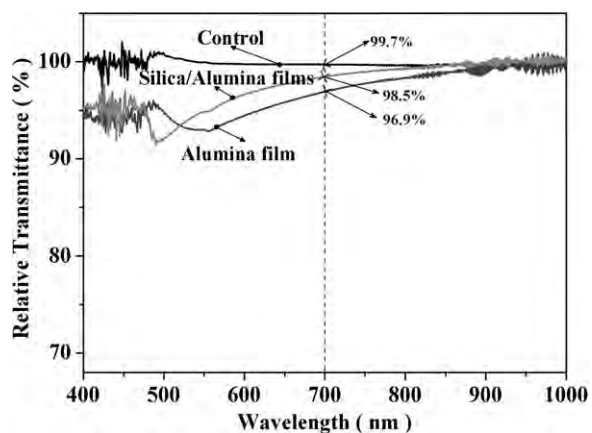


Fig. 6. Optical transmittance of polyimide samples covered with inorganic films with untreated polyimide foil background measurement.

wavelength of 700 nm, the transmittances are 76.0%, 74.6% and 73.1% for the untreated substrate and samples covered with multilayer silica/alumina films and single alumina film, respectively. The optical transmittance of the multilayer silica/alumina films remains similar to that of the control polyimide foil. As shown in Fig. 6, the polyimide foils with protective films maintain more than 90% of the polymer substrate's optical transmittance, and the transmittance is slightly enhanced by the multilayer silica/alumina films contrasting to the single alumina film. The relative optical transmittances of multilayer silica/alumina films and single alumina film are 98.5% and 96.9%, respectively. The high transmittance of multilayer films is suitable for a variety of applications in optical electronic devices where a high transparency is required, so as to minimize the loss of incident light passing through the films. The predominant factor controlling the optical transmission seems to be the formation of new material of $\text{Al}_2\text{O}_3\cdot\text{SiO}_2$. The results demonstrate that plasma implantation and deposition has a slight influence on optical properties of polyimide foil, and the FVAPIID method can fabricate multilayer inorganic silica/alumina films on polyimide with excellent optical transmittance.

3.4. AO erosion of multilayer silica/alumina films analysis

The AO exposure tests were carried out using a ground-based AO effects simulation facility. Polyimide samples were exposed to a hyperthermal AO flux of 2.02×10^{15} atoms $\text{cm}^{-2} \text{s}^{-1}$. The longest exposure time is 21 h and the AO fluence is up to 1.527×10^{20} atoms cm^{-2} . Fig. 7 shows the surface morphologies of PIs with different surface conditions after AO exposure. The polyimide without protecting was severely eroded. The carpet morphology was commonly observed after AO erosion. The erosion holes showed an initiation center and had a size of about $10 \mu\text{m}$ as shown in Fig. 7(a). This was due to that the trapped AO reacts more readily with the weaker polymer bonds [26]. The AO diffused into the polymer and reacted with some elements such as carbon, nitrogen, and hydrogen to form gases and blisters, resulting in the formation of the feature [26,27]. Generally the damage of PIs first occurred on the top surface, thus affecting its morphology, and then continued to the bulk. The sample covered with single alumina film was also eroded, and the surface turned to be scraggly as shown in Fig. 7(b). This was because that some polymer segments existed in the alumina film, and these organic components would react with AO during exposure. Some volatile products carried mass away from the alumina film [28]. In contrast, the polyimide sample covered with multilayer silica/alumina films was shielded from the AO erosion, and demonstrated the smooth surface without visible damage (see Fig. 7(c)). This means the higher anti-AO-erosion capability. Accordingly, the multilayer silica/alumina films still maintains a smooth surface in spite of slightly yellowish shade.

4. Discussion

The high mechanical stability and slight change of surface morphology of polyimide covered with multilayer silica/alumina films showed that the technique was an effective method to protect PIs against AO erosion. With the energetic ion bombarding, the interface composition was mixed into the matrix which improved the adhesion due to the function of ion stitching effect [29] and decreased the residual stress in which the films were grown in densely packed structures [30]. Meanwhile, the ion implantation with high energy applied mechanical interlocking [31] and enough near distance between the reacting groups for chemical bonding [32], and then enhanced the interface adhesion [33,34]. Owing to the excellent adhesion, the multilayer silica/alumina films could avert micro-cracks caused by the mechanical folding. Under the

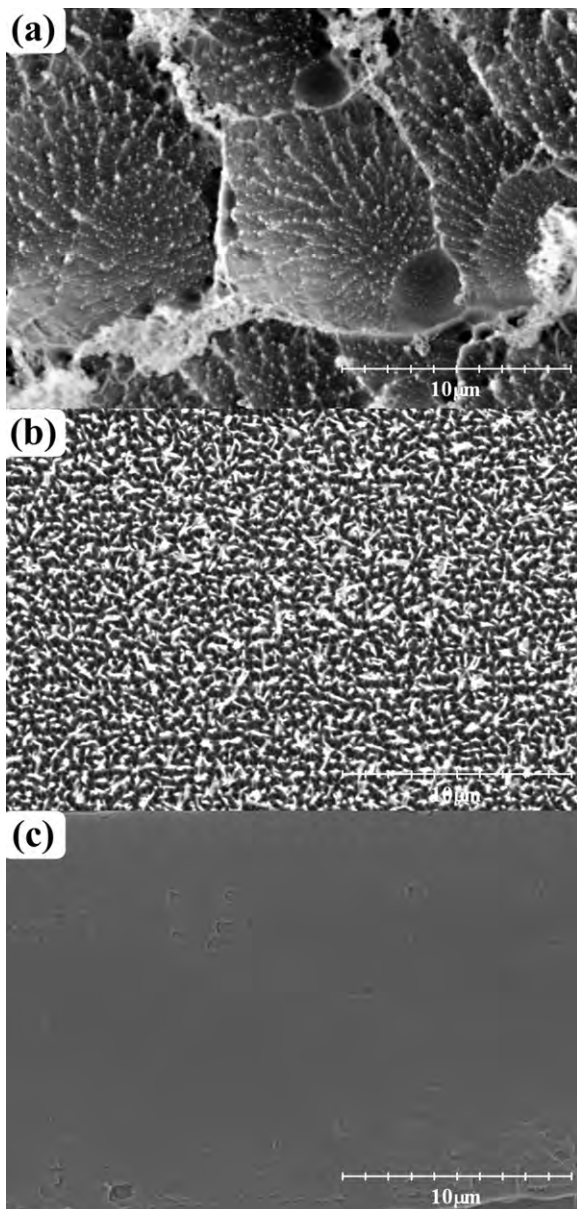


Fig. 7. Characteristic erosion patterns of the polyimide samples with different surface conditions: (a) control polyimide, (b) single alumina film, and (c) multilayer silica/alumina films.

following influence of Si ion implantation, the preventive alumina was induced to form new $\text{Al}_2\text{O}_3 \cdot \text{SiO}_2$ material. The transmittance of multilayer films was enhanced, which was beneficial to the maintenance of the optical performance of polyimide substrate. Attributed to the stress balance of the multilayer structure, the anti-AO erosion performance is enhanced. The silica/alumina layers can provide long-term protection for the organic PIs which were applied to thermal control system of spacecrafts in LEO.

5. Conclusion

In the paper, multilayer inorganic silica/alumina films were fabricated by FVAPIID for protection against AO in low Earth orbit environment. The multilayer films presented the unique mechanical stability, demonstrating that balanced internal stresses and

interconnected bonding structures were crucial for enhancing mechanical stability. The effect of AO on the degradation of polyimide samples with different surface conditions was demonstrated. Polyimide film revealed significant erosion, including formation of carpet morphology. However, the polyimide sample with multilayer films showed better resistance to AO erosion. The FVAPIID process will be promising for fabricating the inorganic protective film on polymer substrate for anti-AO erosion.

Acknowledgments

The work was jointly supported by the National Natural Science Foundation of China (No. 50904020), the Science and Technology Innovation Research Project of Harbin for Young Scholar (No. 2009RFQXG050), the Fundamental Research Funds for the Central Universities (No. HIT. NSRIF. 2012007) and the China Postdoctoral Science Foundation (Nos. 20090460883 and 201003419).

References

- [1] R. Verker, E. Grossman, I. Gouzman, N. Eliaz, *Polymer* 48 (2007) 19–24.
- [2] R. Verker, E. Grossman, N. Eliaz, *Acta Mater.* 57 (2009) 1112–1119.
- [3] H. Shimamura, T. Nakamura, *Polym. Degrad. Stabil.* 95 (2010) 21–33.
- [4] F. Awaja, J.B. Moon, S. Zhang, M. Gilbert, C.G. Kim, P.J. Pigram, *Polym. Degrad. Stabil.* 95 (2010) 987–996.
- [5] Y.H. Choi, X. Bulliard, A. Benayad, Y. Leterrier, J.A.E. Manson, K.H. Lee, D. Choi, J.J. Park, J. Kim, *Acta Mater.* 58 (2010) 6495–6503.
- [6] J. Li, Y. Han, *Langmuir* 22 (2006) 1885–1890.
- [7] M. Deepa, A.K. Srivastava, S. Lauterbach, Govind, S.M. Shivaprasad, K.N. Sood, *Acta Mater.* 55 (2007) 6095–6107.
- [8] P. Mandlik, J. Gartside, L. Han, L.C. Cheng, S. Wagner, J.A. Silvernail, R.Q. Ma, M. Hack, J.J. Brown, *Appl. Phys. Lett.* 92 (2008) 103309.
- [9] P.F. Garcia, R.S. Mclean, M.H. Reilly, M.D. Groner, S.M. George, *Appl. Phys. Lett.* 89 (2006) 031915.
- [10] S. Kwak, J. Jun, E.S. Jung, *Langmuir* 25 (2009) 8051–8055.
- [11] P.C. Ma, W. Nie, Z.H. Yang, P.H. Zhang, G. Li, Q.Q. Lei, L.X. Gao, X.L. Ji, M.X. Ding, *J. Appl. Polym. Sci.* 108 (2008) 705–712.
- [12] P.C. Chiang, W.T. Whang, M.H. Tsai, S.C. Wu, *Thin Solid Films* 447–448 (2004) 359–364.
- [13] Y. Kong, H.W. Du, J.R. Yang, D.Q. Shi, Y.F. Wang, Y.Y. Zhang, W. Xin, *Desalination* 146 (2002) 49–55.
- [14] F. Xiao, K. Wang, M.S. Zhan, *Appl. Surf. Sci.* 256 (2010) 7384–7388.
- [15] M.H. Tsai, S.L. Huang, P.J. Chen, P.C. Chiang, D.S. Chen, H.H. Lu, W.M. Chiu, J.C. Chen, H.T. Lu, *Desalination* 233 (2008) 232–238.
- [16] M. Nogami, *J. Non-Cryst. Solids* 178 (1994) 320–326.
- [17] I. Jaymes, A. Douy, D. Massiot, J.P. Coutre, *J. Non-Cryst. Solids* 204 (1996) 125–134.
- [18] H.H. Huang, Y.S. Liu, Y.M. Chen, M.C. Huang, M.C. Wang, *Surf. Coat. Technol.* 200 (2006) 3309–3313.
- [19] R. Intrater, G. Lempert, E. Gouzman, Y. Cohen, D.M. Rein, R.L. Khalfin, Hoffman, *High Perform. Polym.* 16 (2004) 249–266.
- [20] M.A. Golub, T. Wydeven, *Polym. Degrad. Stabil.* 22 (1988) 325–338.
- [21] Y.X. Huang, X.B. Tian, S.Q. Yang, P.K. Chu, *Rev. Sci. Instrum.* 78 (2007) 103301.
- [22] J. Kurdi, H. Ardelean, P. Marcus, P. Jonnard, F. Arefi-Khonsari, *Appl. Surf. Sci.* 189 (2002) 119–128.
- [23] M. Ishida, H. Kim, T. Kimura, T. Nakamura, *Sens. Actuators A* 53 (1996) 340–344.
- [24] P. Bruesch, E. Halder, P. Kluge, J. Rhyner, P. Roggwiler, T. Stockmeier, F. Stuki, H.J. Wiesmann, *J. Appl. Phys.* 68 (1990) 2226–2234.
- [25] P. Schuler, H.B. Mojazza, R. Haghighat, *High Perform. Polym.* 12 (2000) 113–123.
- [26] V.E. Skurat, E.A. Barbashev, Y.I. Dorofeev, A.P. Nikiforov, M.M. Gorelova, A.I. Pertsyn, *Appl. Surf. Sci.* 92 (1996) 441–446.
- [27] D. He, M.N. Bassim, *J. Mater. Sci.* 33 (1998) 3525–3528.
- [28] Y.X. Huang, X.B. Tian, S.X. Lv, S.Q. Yang, R.K.Y. Fu, P.K. Chu, J.S. Leng, Y. Li, *Appl. Surf. Sci.* 257 (2011) 9158–9163.
- [29] I.H. Tan, M. Ueda, R.S. Dallaqua, N.R. Demarquette, L. Gengembre, *Plasma Process. Polym.* 4 (2007) S1081–S1085.
- [30] Y.F. Zhang, Q. Chen, Z.D. Wang, G.Q. Zhang, Y.J. Ge, *Surf. Coat. Technol.* 201 (2007) 5190–5193.
- [31] Y.X. Huang, X.B. Tian, S.Q. Yang, R.K.Y. Fu, P.K. Chu, *Appl. Surf. Sci.* 253 (2007) 9483–9488.
- [32] L.P. Buchwalter, *J. Adhes. Sci. Technol.* 4 (1990) 697–721.
- [33] W.J. Lee, Y.S. Lee, S.K. Rha, Y.J. Lee, K.Y. Lim, Y.D. Chung, C.N. Whang, *Appl. Surf. Sci.* 205 (2003) 128–136.
- [34] B.A. Latella, G. Triani, P.J. Evans, *Scripta Mater.* 56 (2007) 493–496.